Linear Filtering of Images Based on Properties of Vision

V. Ralph Algazi, Gary E. Ford*, and Hong Chen
CIPIC, Center for Image Processing and Integrated Computing
University of California, Davis
Davis, CA 95616

EDICS: IP 1.2 Filtering

November 1994

Abstract

The design of linear image filters based on properties of human visual perception has been shown to require the minimization of criterion functions in both the spatial and frequency domains. In this correspondence, we extend this approach to continuous filters of infinite support. For low pass filters, this leads to the concept of an ideal low pass image filter which provides a response that is superior perceptually to that of the classical ideal low pass filter.

1 Introduction

The use of hard cutoff (ideal) low pass filters in the suppression of additive image noise is known to produce ripples in the response to sharp edges. For high contrast edges, human visual perception fairly simply determines acceptable filter behavior. Ripples in the filter response are visually masked by the edge, so that the contrast sensitivity of the visual system decreases at sharp transitions in image intensity and increases somewhat exponentially as a function of the spatial distance from the transition.

Algorithmic procedures using properties of human vision have been described for over 20 years [1]. The development of adaptive methods of image enhancement and restoration, based on the use

*Corresponding author; Email: ford@ece.ucdavis.edu; Telephone: 916-752-2387; Fax: 916-752-8894

of a masking function, measure spatial detail to determine visual masking [2,3]. In active regions of the image, visual masking is high, relative noise visibility is low, and the filter applied is allowed to pass more noise until the subjective visibility is equal to that in flat areas.

Whether the filter is adaptive or not, the design of the linear filter to be applied is a critical issue. Hentea and Algazi [4] have demonstrated that the first perceptible image distortions due to linear filtering occur at the major edges and thus, worst case design for visual appearance should be based on edge response. They developed a filter design approach based on the minimization of a weighted sum of squared-error criterion functions in both the spatial and frequency domains. In the spatial domain, the weighting is by a visibility function, representing the relative visibility of spatial details as a monotonically increasing function of the distance from an edge. This visibility function, determined experimentally from the visibility of a short line positioned parallel to an edge, was also found experimentally to predict satisfactorily the visibility of ripples due to linear filters [4].

In the following, we extend the work of Hentea and Algazi by considering the design and properties of one-dimensional continuous filters of infinite support (two-dimensional filters are generated by 1D to 2D transformations). We obtain a new formal result on the low pass filter of infinite support which is optimal for images. It establishes the limiting performance that digital filters of finite complexity can only approximate.

2 Design of One-Dimensional Filters for Images

The basic trade off in the design approach of Algazi and Hentea [4] is maintaining image quality while reducing unwanted artifacts or noise. The image quality is measured by spatial domain criterion function for the visibility of ripples in the vicinity of edges

$$I_1 = \int_{-\infty}^{\infty} w_1^2(x)[\hat{u}(x) - u(x)]^2 dx \tag{1}$$

where $u(x)$ is a unit step input producing the filter response $\hat{u}(x) = u(x) * h(x)$, where $h(x)$ is the point spread function of the filter, $*$ denotes convolution and $w_1(x)$ is a spatial weighting function, chosen to be the visibility function

$$w_1(x) = 1 - a^{|x|} \tag{2}$$

The frequency domain criterion function for the reduction of unwanted artifacts and noise is

$$I_2 = \int_{-\infty}^{\infty} W_2^2(f)|H(f) - H_d(f)|^2 df, \tag{3}$$

where $H_d(f)$ is the desired filter frequency response and $W_2(f)$ is the frequency-domain weighting function. Hentea and Algazi minimized I_1 under a constraint on I_2, but we now minimize the equivalent criterion $J(\alpha) = \alpha I_1 + (1-\alpha)I_2$ where α controls the relative weights of the two criteria, with $0 \leq \alpha \leq 1$.

To develop the optimality condition, (1) is expressed in the frequency domain using Parseval's relation, the transform of a zero-mean step is used, and calculus of variations is applied to the criterion J, resulting in the condition

$$\alpha \left\{ W_1(f) * \left[\frac{H(f) - 1}{j2\pi f} \right] \right\} = (1-\alpha) j2\pi f W_2^2(f)[H(f) - H_d(f)] \tag{4}$$

Substituting the spatial weighting function of (2), with Fourier transform

$$W_1(f) = \delta(f) - \frac{2b}{b^2 + (2\pi f)^2} \tag{5}$$

with $b = -\ln a$, (4) becomes

$$H(f) = \frac{1}{\beta(2\pi f)^2 W_2^2(f)} \left\{ (2\pi f)^2 W_2^2(f) H_d(f) + \left[\frac{b^2}{b^2 + (2\pi f)^2} + j2\pi f \left[\frac{2b}{b^2 + (2\pi f)^2} * \frac{H(f)}{j2\pi f} \right] \right] \right\} \tag{6}$$

where $\beta = (1-\alpha)/\alpha$. This is a linear Fredholm integral equation of the second kind and a discussion of the solution of this equation in terms of eigenfunctions of an equation of similar form arising from a related approach to filter design is given in [5]. That approach is practically useful only if the solution to the homogeneous equation related to (6) is known in closed form or tabulated, which is not the case for our problem. Thus, in the design examples discussed below, we apply a series solution.

3 Low Pass Image Filter Design

For a low pass image filter, the desired frequency response is

$$H_d(f) = \begin{cases} 1 & |f| \leq f_c \\ 0 & |f| > f_c \end{cases} \tag{7}$$

where f_c is the filter cutoff frequency. We choose $W_2(f)$ to weight the stopband response only

$$W_2(f) = \begin{cases} 0 & |f| \leq f_c \\ 1 & |f| > f_c \end{cases} \tag{8}$$

The conditions of (7) and (8) are applied to the integral equation (6). The resulting equation is solved with the Neumann series solution, an iterative approach in which an approximation to $H(f)$ used in the convolution integral on the right-hand side of (6) generates the next approximate solution. Let the kth approximation to $H(f)$ be $\hat{H}_k(f)$, then the $(k+1)$th approximation is

$$\hat{H}_{k+1}(f) = H_u(f)\left[\frac{b^2}{b^2 + (2\pi f)^2} + j2\pi f\left[\frac{2b}{b^2 + (2\pi f)^2} * \frac{\hat{H}_k(f)}{j2\pi f}\right]\right] \tag{9}$$

where

$$H_u(f) = \begin{cases} 1 & |f| \leq f_c \\ \dfrac{1}{1 + \beta(2\pi f)^2} & |f| > f_c \end{cases} \tag{10}$$

The initial condition for the iterative solution is $\hat{H}_0(f) = H_u(f)$. In the examples considered, we observed that the solutions converged to an accuracy of three decimal places in only eight iterations, convergence was not strongly affected by the initial condition, and there was no indication that the solution was not unique. A discussion of convergence for a series solution to a similar integral equation is given in [5].

As an example, consider the design of a low pass filter with cutoff frequency $f_c = 0.15$ (normalized) and $\alpha = 0.6$. Normalizing the viewing distance to six times the image height, the resulting angular increment is 1.116 minutes of arc per pixel and the appropriate value for a in $w_1(x)$ is 0.72 ($b = 0.33$) [4]. The ripples in the step response of the resulting figure, shown in Figure 1, are strongly suppressed. The frequency response of filter is shown in Figure 2.

[Figure 1 about here.]

[Figure 2 about here.]

The plot showing the tradeoff between I_1 and I_2 as a function of α in Figure 3 can be used to choose α to meet specifications on I_1 or I_2. Note the large decrease in the frequency domain rejection that is required for a small improvement in spatial domain response.

[Figure 3 about here.]

Of independent interest is the ideally bandlimited low pass image filter, which results from setting $\alpha \to 0$ or $\beta \to \infty$. The filter design in this case is equivalent to minimizing spatial domain criterion I_1 under the constraint that the stopband energy of I_2 be zero.

The form of (9) remains the same, but $H_u(f)$ (and the initial condition $\hat{H}_0(f)$) becomes the frequency response of the classical ideal low pass filter

$$H_u(f) = \begin{cases} 1 & |f| \leq f_c \\ 0 & |f| > f_c \end{cases} \tag{11}$$

The step response of an example filter with cutoff frequency $f_c = 0.15$ (normalized) and $a = 0.72$, shown in Figure 1, has a ripple response that is better than that of the classical ideal low pass filter. The spatial error integral I_1 for the ideal image low pass filter is 45% less than that for the classical ideal low pass filter. The filter frequency response for this example is shown in Figure 4.

[Figure 4 about here.]

4 Low Pass Filter Examples

To illustrate the properties of the low pass image filters discussed in the section above, we consider two-dimensional FIR approximations of the design examples and compare performance with that of an equiripple filter on a noisy image. To ensure ease of comparison of the halftone reproductions in a journal publication, a test image with substantial distortion was chosen. The results clearly extend to images of lower contrast and smaller distortions. High frequency noise was added to the original image of Figure 5a by high pass filtering noise with a uniform distribution, producing the noisy image shown in Figure 5b, having peak signal-to-noise ratio (PSNR) of 8.22dB.

The noisy image was filtered by an equiripple low pass filter which approximates an ideal low pass filter, and a low pass image filter design with our approach, each having the same maximum deviation in the stopband and cutoff frequency $f_c = 0.15$ (normalized frequency). The low pass image filter is based on the one-dimensional design with $\alpha = 0.6$, having frequency response shown in Figure 2. The applied filters are two-dimensional circularly symmetric, obtained from one-dimensional filters by McClellan's transformation [6]. The equiripple filter response in in Figure 5c shows strong ripple responses at major transitions and it produces a PSNR of 25.5dB. The low pass image filter response in Figure 5d has suppressed the ripples and produced an improved PSNR of 32.3dB. Thus, the low pass image filter is superior perceptually and it provides better noise reduction.

[Figure 5 about here.]

The ripple responses of the low pass filters are compared in the checkerboard images of Figure 6. Figures 6b through 6d show the responses of filters having a cutoff frequency $f_c = 0.15$ (normalized frequency). The response of a classical ideal low pass filter is shown in Figure 6b, showing very strong ripple response. The response of the ideal low pass image filter of Section 3, with $\alpha = 0$ and having the frequency response of Figure 4 is shown in Figure 6c, where the ripples have decreased substantially. Finally, in the response to the low pass image filter from Section 3, with frequency response shown in Figure 2 for $\alpha = 0.6$, the ripples are difficult to perceive.

[Figure 6 about here.]

5 Discussion and Conclusions

We have reconsidered a method for the design of linear filters for image processing based on properties of the human visual system, which involves the minimization of criterion functions in both the spatial and frequency domains. We have extended this work by obtaining new theoretical results by considering continuous filters of infinite support.

An important limiting result for an ideal low pass image filter having infinite support has been obtained. This ideal low pass image filter is greatly superior perceptually to the classical low pass filter and provides a design target for the important problems of image sampling and interpolation.

We have found that interpolation filters designed with this approach provide better results than bicubic filters that approximate classical ideal low pass filters [7].

Acknowledgment

This work was supported by the University of California MICRO Program, Grass Valley Group, Pacific Bell, Lockheed, and Hewlett Packard.

References

[1] B. R. Hunt, "Digital image processing," *IEEE Proceedings*, vol. 63, pp. 693–708, 1975.

[2] G. L. Anderson and A. N. Netravali, "Image restoration based on a subjective criterion," *IEEE Trans. Syst., Man, and Cyber.*, vol. 6, no. 12, pp. 845–853, 1976.

[3] A. Katsaggelos, "Iterative image restoration algorithms," *Optical Engineering*, vol. 28, pp. 735–748, 1989.

[4] T. A. Hentea and V. R. Algazi, "Perceptual models and the filtering of high-contrast achromatic images," *IEEE Trans. Systs., Man, and Cyber.*, vol. 14, no. 2, pp. 230–246, 1984.

[5] V. R. Algazi and M. Suk, "On the frequency weighted least-square design of finite duration filters," *IEEE Trans. Circuits and Systems*, vol. 22, no. 12, pp. 943–953, 1975.

[6] J. H. McClellan, "The design of two-dimensional digital filters by transformations," *Proc. 7th Annual Princeton Conf. Inform. Sci. and Syst.*, pp. 247–251, 1973.

[7] H. Chen and G. E. Ford, "An FIR image interpolation filter design method based on properties of human vision," in *Proc. IEEE Intl. Conf. Image Proc.*, vol. III, pp. 581–585, 1994.

List of Figures

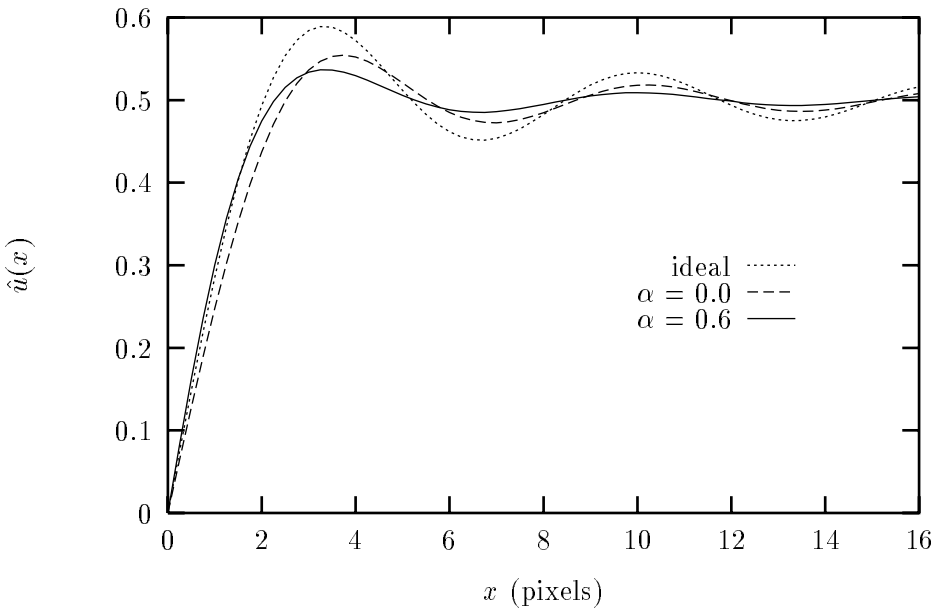

Figure 1: Comparison of filter step responses.

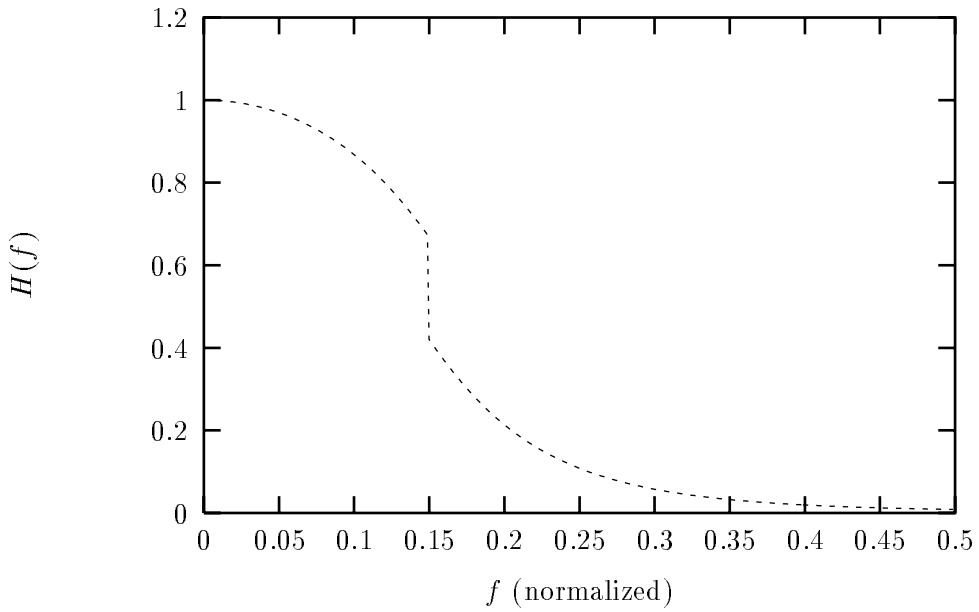

Figure 2: Low pass image filter frequency response for $\alpha = 0.60$.

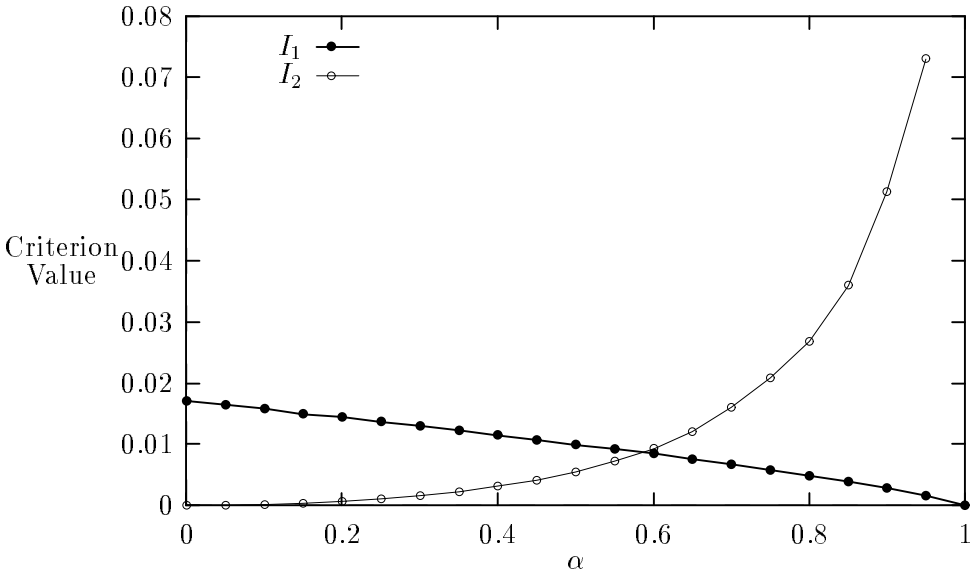

Figure 3: Design criteria I_1 and I_2 as a function of α.

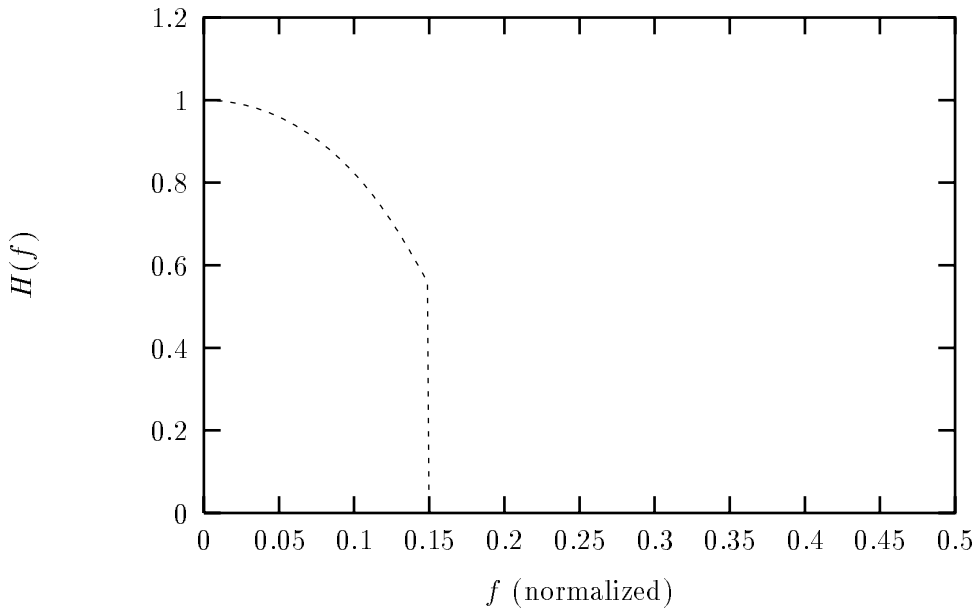

Figure 4: Frequency response for ideal low pass image filter, $\alpha = 0$.

Figure 5: Low-pass filtering: (a) Original image; (b) Noisy image; (c) Noisy image processed with an equiripple low-pass filter; (d) Noisy image processed with a low pass image filter, $\alpha = 0.6$.

a	b
c	d

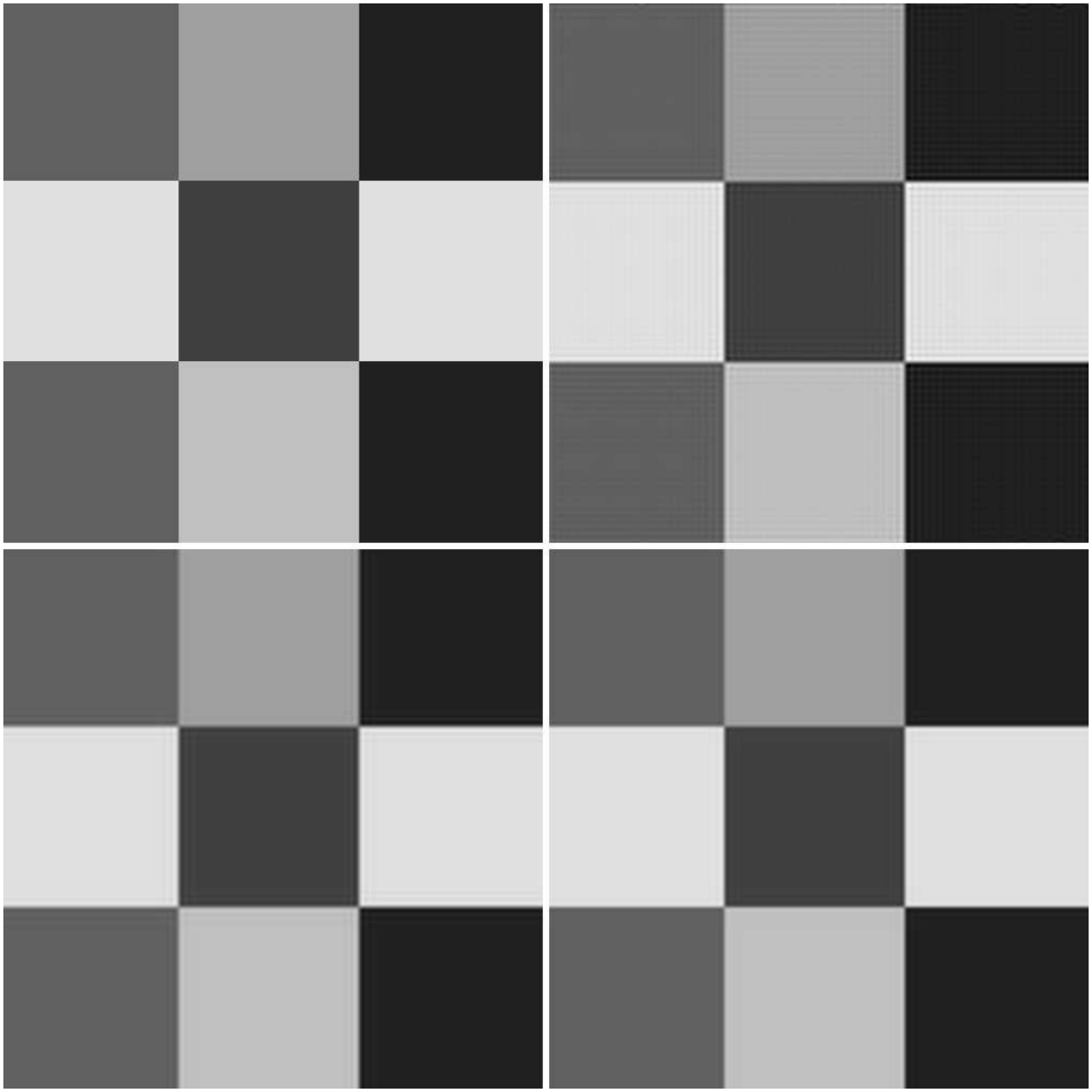

Figure 6: Image filtering by low pass filters. (a) Original image; (b) Filtered with classical ideal low pass filter; (c) Filtered with ideal low pass image filter, $\alpha = 0$; (d) Filtered with low pass image filter, $\alpha = 0.6$.

a	b
c	d